Proceeding of the 7th International Symposium on Artificial Intelligence, Robotics and Automation in Space:
i-SAIRAS 2003, NARA, Japan, May 19-23, 2003

Design and control of three-dimensional trajectory for a space robot flying around a target satellite in consideration of a change in the thrust

Masayuki Sugahara Yasuhiro Masutani Fumio Miyazaki

Department of Systems and Human Science
Graduate School of Engineering Science, Osaka University
1-3, Machikaneyama-cho, Toyonaka, Osaka 560-8531, Japan
sugahara@robotics.me.es.osaka-u.ac.jp

Keywords Space robot, Flyaround, Extended Kalman filter, LOS angle, VIC controller

Abstract

This paper presents a method of designing and keeping three-dimensional flyaround trajectory for a space robot (chaser) flying periodically around a troubled satellite (target) on a circular orbit around the earth. The trajectory is designed by considering orbital dynamics of the chaser represented by the Hill's equation. An optimal feedback control scheme for the thrust is proposed to maintain trajectory in the presence of disturbances. The extended Kalman filter is employed to estimate state and control variables which are not available for measurement. Simulation results that verify the trajectory keeping capability of the proposed thrust control are also presented.

1 Introduction

In order to provide services for an Earth-orbiting satellite, it is desirable to be able to use a fully autonomous servicing space robot that flies around it, observes it carefully, and performs distant operations. In practice, NASA developed a prototype remotely controlled free-flying television camera, AERCam Sprint (Autonomous Extravehicular Activity Robotic Camera Sprint), so as to inspect large scale structures such as the International Space Station and experimentally examined its performance in a Space Shuttle mission STS-87 (Space Transportation System-87) in 1997 [1][2]. NASDA is planning to develop "Eyeball Satellite" flying around its mother satellite and sending inspected data to the Earth [3].

Close circumnavigation is an important function indispensable for servicing space robot. Conventional flyaround maneuvers including these two examples use circular, elliptical, or rectilinear trajectories relative to the target satellite. Future space service missions are driving the need for small, low cost satellites whose motion relative to the target satisfies the following conditions;

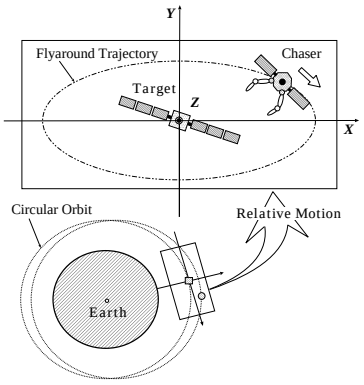

Fig. 1 C-W coordinate frame

- The flyaround period is variable (especially shorter than the Earth-orbiting period of the target).
- The distance from a target satellite does not vary much.
- The amount of fuel consumption is small.
- The trajectory can be maintained under disturbances by simple thruster control

On the assumption that the on-board equipment on the chaser does not have sufficient computing power and the chaser can not perform the flyaround maneuver in cooperation with the target, the authors proposed two-dimensional (in-plane) flyaround trajectories and an impulsive thrust control scheme to hold the trajectory under disturbances[4].

However, 2-impulse flyaround trajectory does not allow the flyaround period full of variety, because the flyaround period cannot be chosen independently of the trajectory shape. To overcome this limitation, we propose a three-dimensional (out-of-plane) flyaround

trajectory, named "4-impulse flyaround", which satisfies the above four conditions. Moreover, we consider the situation that the thrust of the thrusters is unknown, supposing that the acceleration given to the chaser by the thrust deviates from the nominal value due to degradation of the thrusters caused by the prolonged use and a change of mass owing to a reduction in fuel. We propose a method of estimating the thrust, which is incorporated into the impulse thrust control scheme.

This paper is organized as follows. In **Sec.2**, we investigate the flyaround orbit for a servicing space robot (chaser) flying around a troubled satellite using the linearized relative orbital dynamics known as Hill's equation. Three-dimensional flyaroud trajectory satisfying the above conditions can be obtained using impulsive thrust, which is shown in **Sec.3**. An optimal feedback control scheme for the thrust is given in **Sec.4** to maintain this trajectory in the presence of disturbances. **Sec.5** describes how to estimate state variables necessary for the feedback control using Extended Kalman Filter, assuming that the direction of the target is the only variables the chaser can observe. In **Sec.6**, assuming that the thrust of the thrusters is unknown, a method of estimating the thrust is proposed. Simulations in **Sec.7** illustrate the performance of the proposed methods under practical conditions including the deviation of the thrust from its nominal value. Concluding remarks are made in **Sec.8**.

2 Relative Motion on Circular Orbit

Let us consider an orthogonal coordinate frame X, Y, and Z which moves together with the target on the circular orbit of the earth as shown in Fig. 1. Its origin coincides with the target position, Y axis is directed to the center of the earth, Z axis is orthogonal to the orbital plane, and X axis is defined according to the right-hand rule. This coordinate frame is rotating on a circular orbit of the target with the orbital angular velocity ω around Z axis.

Because the relative distance between the chaser and the target can be assumed to be sufficiently small in comparison with a radius of the target's orbit, the linearized differential equations of relative motion is obtained, which is called the Hill's equation. Introducing the normalized time $\tau = \omega t$ and its derivatives as $\frac{d}{d\tau}() = \dot{()}$ and $\frac{d^2}{d\tau^2} = \ddot{()}$, the equation is written as follows.

$$\ddot{x} = 2\dot{y} + \alpha_x \quad (1)$$

$$\ddot{y} = -2\dot{x} + 3y + \alpha_y \quad (2)$$

$$\ddot{z} = -z + \alpha_z \quad (3)$$

where $\alpha_i = A_i/\omega^2$ $(i = x, y, z)$. A_i is the acceleration applied by thrust. The C-W solution in case of free motion($\alpha_x = \alpha_y = \alpha_z = 0$) can be written in the following forms.

$$\begin{bmatrix} x(\tau) \\ y(\tau) \\ z(\tau) \end{bmatrix} = \begin{bmatrix} a + 2c\sin(\tau + \phi) - b\tau \\ -2/3b + c\cos(\tau + \phi) \\ \dot{z}_0 \sin(\tau) + z_0 \cos(\tau) \end{bmatrix} \quad (4)$$

where a, b, c, and ϕ are constants determined from the initial conditions.

3 Design of Flyaround Trajectories

3.1 Free Motion

In case of free motion, the chaser moves in an out-of-plane circular trajectory written by

$$\begin{bmatrix} x(\tau) \\ y(\tau) \\ z(\tau) \end{bmatrix} = \begin{bmatrix} 2y_0 \sin\tau \\ y_0 \cos\tau \\ \dot{z_0} \sin\tau \end{bmatrix} \quad (5)$$

Though this trajectory which crossing the orbital plane at an angle of 60 degrees does not need any fuel consumption, the flyaround period τ_f is fixed as $\tau_f = 2\pi$, the orbital period of the target.

3.2 Two-Dimensional Flyaround

3.2.1 2-Impulse Flyaround Thrusting on Y Axis

We proposed "2-impulse flyaround thrusting on Y axis" which is performed using impulsive thrusts of only twice for one flyaround period as shown in Fig. 2 [4]. The flyaround trajectory given by this method is restricted on a plane. Variations in the trajectory shape in terms of the ratio between the flyaround period and the orbital period $k = \tau_f/2\pi$ are shown in Fig. 3. Since the trajectory shape depends on the flyaround period, it is not suitable for the observation of the target.

3.2.2 2-Impulse Flyaround Thrusting on X Axis

In order to overcome the limitation of the above-mentioned 2-impulse flyaround, we extend it to a three-dimensional version. Before presenting solutions, we explain "2-impulse flyaround thrusting on X axis" as shown in Fig. 4. Letting the flyaround period be τ_f $(\tau_f < 2\pi)$, the trajectory is expressed as follows.

$$\begin{bmatrix} x(\tau) \\ y(\tau) \end{bmatrix} = \begin{cases} d \begin{bmatrix} -\frac{3}{8}\tau_f \cos\frac{\tau_f}{4} - 2\sin(\tau' - \frac{\tau_f}{4}) + \frac{3}{2}\tau' \cos\frac{\tau_f}{4} \\ \cos\frac{\tau_f}{4} - \cos(\tau' - \frac{\tau_f}{4}) \end{bmatrix} & (0 < \tau' < \frac{\tau_f}{2}) \\ d \begin{bmatrix} \frac{9}{8}\tau_f \cos\frac{\tau_f}{4} + 2\sin(\tau' - \frac{3\tau_f}{4}) - \frac{3}{2}\tau' \cos\frac{\tau_f}{4} \\ -\cos\frac{\tau_f}{4} + \cos(\tau' - \frac{3\tau_f}{4}) \end{bmatrix} & (\frac{\tau_f}{2} < \tau' < \tau_f) \end{cases}$$

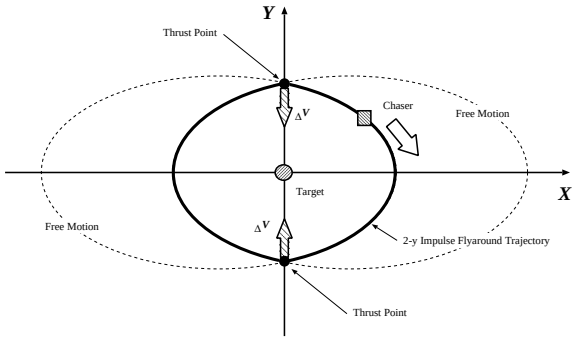

Fig. 2 2-Impulse Flyaround Trajectory thrusting on Y axis

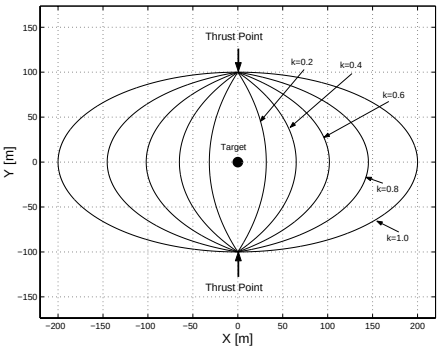

Fig. 3 Relation of 2-Impulse Flyaround Trajectory thrusting on Y axis to normalized period

where

$$d = \frac{x_0}{2\sin\frac{\tau_f}{4} - \frac{3}{8}\tau_f\cos\frac{\tau_f}{4}}$$
$$\tau' = \mathrm{mod}(\tau, \tau_f)$$

and mod means a modulus function of real number. Variations in the trajectory shape in terms of the ratio between the flyaround period and the orbital period $k = \tau_f/2\pi$ are shown in Fig. 5.

The ratio between the distance to the target on X axis and on Y axis is expressed as follows.

$$\frac{y_{max}}{x_0} = \frac{x_0}{2\sin\frac{\tau_f}{4} - \frac{3}{8}\tau_f\cos\frac{\tau_f}{4}}(1-\cos\frac{\tau_f}{4}) \qquad (6)$$

The sum of normalized by velocity changes ΔV is described by

$$\frac{\tau_f \Delta V}{x_0} = \frac{\tau_f}{\tan\frac{\tau_f}{4} - \frac{3}{16}\tau_f} \qquad (7)$$

3.3 Three-Dimensional Flyaround

Three-dimensional trajectory is composed of the in-plane motion ($X-Y$ plane) and the motion in the direction of Z axis. Above-mentioned "2-impulse flyaround thrusting on X axis" is adopted as the in-plane motion.

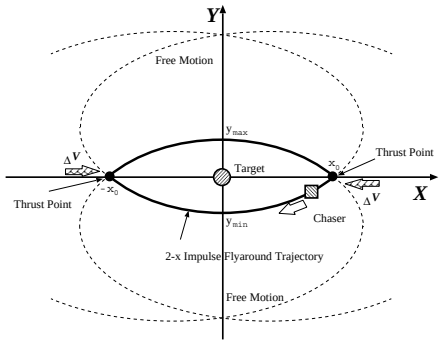

Fig. 4 2-Impulse Flyaround Trajectory thrusting on X axis

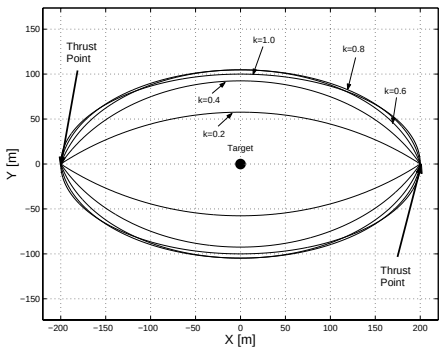

Fig. 5 Relation of 2-Impulse Flyaround Trajectory thrusting on X axis to normalized period

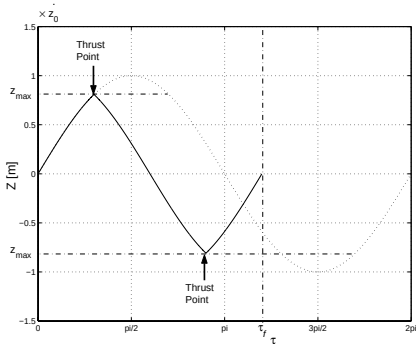

Fig. 6 Motion in the direction of Z axis

3.3.1 Motion in the Direction of Z Axis

Let us consider only the motion in the direction of Z axis. It is a simple harmonic motion in case of free motion. Arbitrary period τ_f is performed using impulsive thrusts of only twice for one period at $\tau = \frac{\tau_f}{4}, \frac{3\tau_f}{4}$ in Fig. 6. C-W equation of this motion is given by

$$\dot{z_0} = \frac{z_{max}}{\sin\frac{\tau_f}{4}} \qquad (8)$$

$$z(\tau) = \begin{cases} \dot{z_0}\sin\tau' & (0 < \tau' < \frac{\tau_f}{4}) \\ -\dot{z_0}\sin(\tau' - \frac{\tau_f}{2}) & (\frac{\tau_f}{4} < \tau' < \frac{3\tau_f}{4}) \\ \dot{z_0}\sin(\tau' - \tau_f) & (\frac{3\tau_f}{4} < \tau' < \tau_f) \end{cases}$$

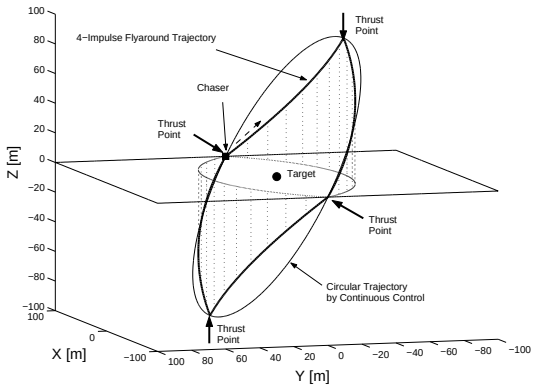

Fig. 7 4 Impulse Flyaround Trajectory

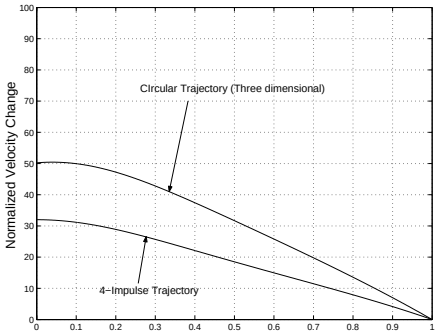

Fig. 8 Normalized Total Velocity to normalized period

The sum of normalized by velocity changes ΔV is expressed by

$$\Delta V = 4\frac{z_{max}}{\tan\frac{\tau_f}{4}} \tag{9}$$

3.4 4-Impulse Flyaround

We propose "4-impulse flyaround" by combining "2-impulse flyaround thrusting on X axis" and the above mentioned motion in the direction of Z axis as shown in Fig. 7. Impulsive velocity changes are performed every quarter of the flyaround period $\tau_f/4$.

"4-impulse flyaround" has the following advantages. The distance between the target and the chaser can be kept almost constant independently of the flyaround period. Moreover, the chaser can be easily thrown into the trajectory, because of the initial point being the same altitude ($y = 0$). The amount of the velocity change is required about 40% less than a circular flyaround trajectory passing through the four thrust points.

4 Trajectory keeping Based on Discrete Modeling

We propose an optimal feedback control scheme for the thrust to maintain the "4-impulse flyaround"

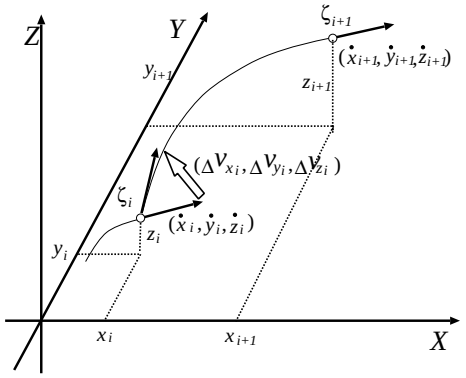

Fig. 9 Discrete State of Impulse Trajectory

trajectory in the presence of disturbances. Considering impulsive thrust at an interval of τ_e, we can obtain the following discrete state equation.

$$\begin{aligned} \boldsymbol{\zeta}_{i+1} &= \boldsymbol{A}_{\tau_e}\boldsymbol{\zeta}_i + \boldsymbol{B}_{\tau_e}\boldsymbol{\nu}_i \qquad (i = 0,\ 1, \cdots) \qquad (10)\\ \boldsymbol{\zeta}_i &= [x(i\tau_e), y(i\tau_e), z(i\tau_e), \dot{x}(i\tau_e), \dot{y}(i\tau_e), \dot{z}(i\tau_e)]^T \\ \boldsymbol{\nu}_i &= [\Delta v_{xi}, \Delta v_{yi}, \Delta v_{zi}]^T \end{aligned}$$

where $\boldsymbol{\zeta}_i \in \mathbf{R}^{6\times 1}$ is the position and velocity vector at the i-th thrusting time and $\boldsymbol{\nu}_i \in \mathbf{R}^{3\times 1}$ is the corresponding velocity change regarded as a control input. For a certain flyaround period τ_f, there exists nominal values $\boldsymbol{\zeta}^*$ and $\boldsymbol{\nu}^*$. Deviations from the nominal state $\boldsymbol{\zeta}^*$ and $\boldsymbol{\nu}^*$ are defined as follows.

$$\Delta\boldsymbol{\zeta}_i = \boldsymbol{\zeta}_i - \boldsymbol{\zeta}_j^* \qquad (i = 0,\ 1, \cdots) \tag{11}$$

$$\Delta\boldsymbol{\nu}_i = \boldsymbol{\nu}_i - \boldsymbol{\nu}_j^* \qquad (i = 0,\ 1, \cdots) \tag{12}$$

Using Eq.(10), the discrete system whose state is $\Delta\boldsymbol{\zeta}_i$ is described by

$$\Delta\boldsymbol{\zeta}_{i+1} = \boldsymbol{A}\Delta\boldsymbol{\zeta}_i + \boldsymbol{B}\Delta\boldsymbol{\nu}_i \tag{13}$$

Since this system is controllable, it can be stabilized by a linear state feedback

$$\Delta\boldsymbol{\nu}_i = -\boldsymbol{F}\Delta\boldsymbol{\zeta}_i \tag{14}$$

where $\boldsymbol{F} \in \mathbf{R}^{3\times 6}$ is a feedback gain matrix determined by LQR for example.

5 Estimation Based on LOS Angle

When controlling a flyaround trajectory using a thruster system on the chaser, the controller needs to know the position and velocity relative to the target. If it is assumed that the sensor based on optical principle is used, the relative angle between the satellites is more easily acquirable than the relative distance. Therefore, in this section, the Kalman filter which observe two LOS (Line of Sight) angles as shown in Fig. 10 is introduced to estimate the whole state variables of the chaser.

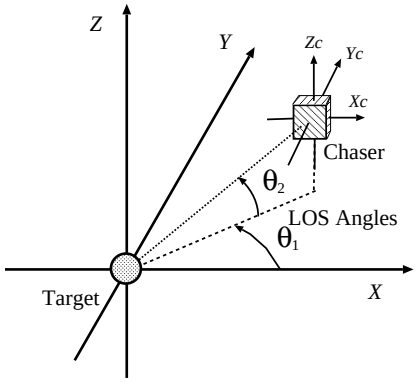

Fig. 10 Observation of the Target from the Chaser

Considering that the filter observe discretely and outputs $\boldsymbol{\eta}$, the discrete system updated at an interval of T is described by

$$\boldsymbol{\xi}[n+1] = \boldsymbol{A}\boldsymbol{\xi}[n] + \boldsymbol{B}\boldsymbol{u}[n] + \boldsymbol{G}\boldsymbol{v}[n] \quad (15)$$

$$\boldsymbol{\eta}[n] = c(\boldsymbol{\xi}[n]) + w[n] \quad (16)$$

$$\boldsymbol{\xi}[n] = [x(nT), y(nT), z(nT), \dot{x}(nT), \dot{y}(nT), \dot{z}(nT)]^T$$

$$\boldsymbol{u}(t) = [\alpha_x(nT), \alpha_y(nT), \alpha_z(nT)]^T$$

$$\boldsymbol{A} = \begin{bmatrix} 1 & 0 & 0 & T & 0 & 0 \\ 0 & 1 & 0 & 0 & T & 0 \\ 0 & 0 & 1 & 0 & 0 & T \\ 0 & 0 & 0 & 1 & 2T & 0 \\ 0 & 3T & 0 & -2T & 1 & 0 \\ 0 & 0 & -T & 0 & 0 & 1 \end{bmatrix}$$

$$\boldsymbol{B} = \begin{bmatrix} 0 & 0 & 0 \\ 0 & 0 & 0 \\ 0 & 0 & 0 \\ T & 0 & 0 \\ 0 & T & 0 \\ 0 & 0 & T \end{bmatrix}, \boldsymbol{G} = \begin{bmatrix} 0 & 0 & 0 \\ 0 & 0 & 0 \\ 0 & 0 & 0 \\ 1 & 0 & 0 \\ 0 & 1 & 0 \\ 0 & 0 & 1 \end{bmatrix}$$

$$c(\boldsymbol{\xi}[n]) = \boldsymbol{\theta}[nT] = \begin{bmatrix} \tan^{-1}\frac{y[nT]}{x[nT]} & \tan^{-1}\frac{z[nT]}{\sqrt{x^2[nT]+y^2[nT]}} \end{bmatrix}$$

where it is assumed that $\boldsymbol{v}$ is an white process noise with average 0 and covariance matrix $\boldsymbol{Q}$ and that w is a white observation noise with average of 0 and covariance matrix $\boldsymbol{R}$.

Since the output model (16) is nonlinear, the extended kalman filter must be used to estimate the state. Linearizing the output model around $\widehat{\boldsymbol{\xi}}[n|n-1]$, the following equation is described by

$$\boldsymbol{\eta}[n] = \boldsymbol{C}[n]\boldsymbol{\xi}[n] + w[n] \quad (17)$$

$$\boldsymbol{C}[n] = \left.\frac{\partial c}{\partial \boldsymbol{\xi}}\right|_{\boldsymbol{\xi}=\widehat{\boldsymbol{\xi}}[n|n-1]}$$

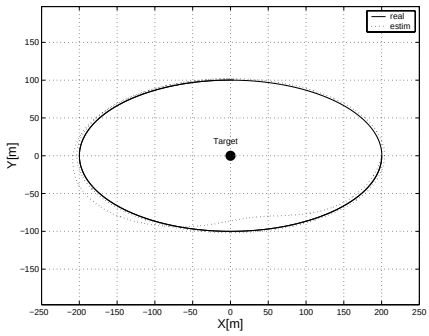

Fig. 11 X-Y Plane

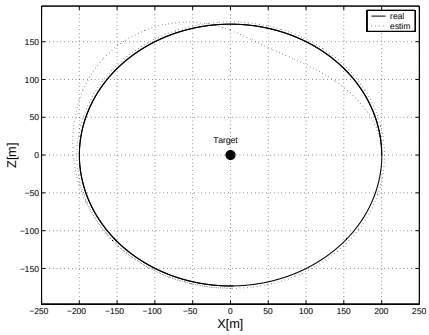

Fig. 12 X-Z Plane

$$= \left[\begin{array}{cccc} -\frac{y}{(x^2+y^2)} & \frac{x}{(x^2+y^2)} & 0 & 0 \\ -\frac{xz}{\sqrt{x^2+y^2}(x^2+y^2+z^2)} & -\frac{yz}{\sqrt{x^2+y^2}(x^2+y^2+z^2)} & 0 & 0 \\ \frac{\sqrt{x^2+y^2}}{(x^2+y^2+z^2)} & 0 & 0 & 0 \end{array} \right]_{\boldsymbol{\xi}=\widehat{\boldsymbol{\xi}}[n|n-1]}$$

There is a problem that the system is not observable on X axis ($y = z = 0$). However, since the moving chaser instantaneity passed the point, we try to apply the extended Kalman filter.

In order to verify the effectiveness of the Kalman filter constituted above, the simulation is performed for the circular trajectory by free motion crossing the orbital plane at an angle of 60 degrees. The updating interval is $T/\omega = 0.1$[s]($\omega = 1.1\times10^{-3}$[rad/s]). In order to clarify the performance of the filter, quite large initial estimation error is given(initial estimated velocity equal to zero). On the other hand, the system noise (standard deviation 2.5×10^{-6} [m/s^2]) and the observation noise (standard deviation 0.1 [deg]) in the simulation model are set to the same as filter model. As results, estimation error decreases initially but small steady deviation remains. We realize that the proposed extended kalman filter is effective in some range especially for flyaround like motion. Although there exists a problem that small steady deviation remains, it can be estimated and solved in **Sec.6.5**.

6 Thrust Estimation

6.1 VIC controller

We adopt the VIC (Velocity Increment Cutoff) as the simplest thrusting method to achieve impulsive velocity change. It is assumed that thrusters are mounted on the chaser in X, Y, and Z directions and controlled independently. Unlike the usual VIC, the thrusters were cut off based on not an accelerometer but the estimated velocity by EKF. The VIC control sequence is as follows.

- The position and velocity of the chaser is estimated from the LOS angle by the EKF at interval T.
- Optimal velocity change is computed by LQR for every impulse interval τ_e using the estimation from EKF.
- VIC is adopted for thruster control. Comparing the estimated velocity by EKF and the desired velocity computed by LQR at interval T, a constant thrust is maintained until the velocity reaches the desired value (Fig. 13).

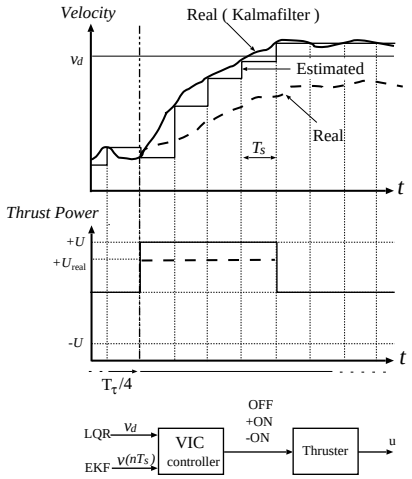

Fig. 13 VIC Controller

6.2 Change in the Thrust

In the proposed method, on the assumption that the thrust and the whole mass of the chaser containing the fuel are known, the state is estimated by EKF[4]. However, there is a possibility that the acceleration given to the chaser by the thrust deviates from the nominal value due to degradation of the thrusters caused by the prolonged use and a change of mass owing to a reduction in fuel. Although the acceleration given to the chaser is changed in the both of cases, in order to make a problem intelligible, it is assumed that the mass is constant and the thrust changes in this paper. In VIC control sequence, the estimated velocity by EKF is based on the nominal value of the thrust. Thus, if the actual thrust of the chaser differs from the nominal value, the estimated velocity by EKF becomes different from the real velocity at cutting off the thruster, then VIC controller cannot perform correctly as shown in Fig. 13. In order to solve the above problem, it is necessary to estimate the thrust.

6.3 Thrusting Motion

The proposed flyaround trajectory is a repetition of thrusting motion for short time and free motion for long time. We take up only one section in the repetition. For simplicity, the motion of the in-plane is considered, because the motion in the direction of Z axis is independent. Letting the position and velocity be state vector $\boldsymbol{\xi} = [x\ y\ \dot{x}\ \dot{y}]^T$, the state just before the thrusting motion, just after the thrusting motion and just before the next thrusting motion are denoted by $\boldsymbol{\xi}_0$, $\boldsymbol{\xi}_1$ and $\boldsymbol{\xi}_2$ respectively. When the thrusters are operated, it is assumed that the acceleration given to the chaser is constant $\boldsymbol{\alpha} = [\alpha_x\ \alpha_y]^T$. Given an initial state $\boldsymbol{\xi}_0$ and constant acceleration $\boldsymbol{\alpha}$, the state after velocity change for time τ is described by

$$\boldsymbol{\xi}' = \boldsymbol{A}(\tau)\boldsymbol{\xi}_0 + \boldsymbol{B}(\tau)\boldsymbol{\alpha} \tag{18}$$

$$\boldsymbol{A} = \begin{bmatrix} 1 & -6\sin\tau + 6\tau & 4\sin\tau - 3\tau & 2 - 2\cos\tau \\ 0 & 4 - 3\cos\tau & 2\cos\tau - 2 & \sin\tau \\ 0 & 6\cos\tau + 6 & 4\cos\tau - 3 & 2\sin\tau \\ 0 & 3\sin\tau & -2\sin\tau & \cos\tau \end{bmatrix}$$

$$\boldsymbol{B} = \begin{bmatrix} 4 - \frac{3}{2}\tau^2 - 4\cos\tau & 2\tau - 2\sin\tau \\ -2\tau + 2\sin\tau & 1 - cos\tau \\ -3\tau + 4\sin\tau & 2 - 2\cos\tau \\ -2 + 2\cos\tau & \sin\tau \end{bmatrix} = \begin{bmatrix} \boldsymbol{B}_x & \vdots & \boldsymbol{B}_y \end{bmatrix}$$

Since thrusters are mounted on the chaser in X and Y directions and controlled independently, the thrusting time τ_x and τ_y on axis X and Y are not necessarily equal. For example, when the chaser moves with the thrust for the thrusting time τ_y ($\geq \tau_x$), the state $\boldsymbol{\xi}_1$ after the time τ_y is described by

$$\begin{aligned} \boldsymbol{\xi}_1 &= \boldsymbol{A}(\tau_y - \tau_x)\{\boldsymbol{A}(\tau_x)\boldsymbol{\xi}_0 + \boldsymbol{B}_x(\tau_x)\alpha_x + \boldsymbol{B}_y(\tau_x)\alpha_y\} \\ &\quad + \boldsymbol{B}_y(\tau_y - \tau_x)\alpha_y \end{aligned}$$

This can be rewritten in the following form.

$$\boldsymbol{M}(\tau_x,\ \tau_y)\boldsymbol{\alpha} = \boldsymbol{\xi}_1 - \boldsymbol{A}(\tau_y)\boldsymbol{\xi}_0 \tag{19}$$

where

$$\begin{aligned} \boldsymbol{M}(\tau_x,\ \tau_y) &= \begin{bmatrix} \boldsymbol{A}(\tau_y - \tau_x)\boldsymbol{B}_x(\tau_x) \\ \boldsymbol{A}(\tau_y - \tau_x)\boldsymbol{B}_y(\tau_x) + \boldsymbol{B}_y(\tau_y - \tau_x) \end{bmatrix}^T \\ &\in \boldsymbol{R}^{4\times 2} \end{aligned}$$

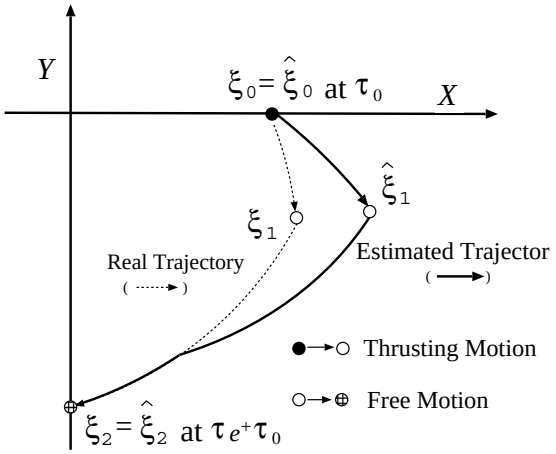

Fig. 14 Related to the relativity based on LOS Angle and Distance

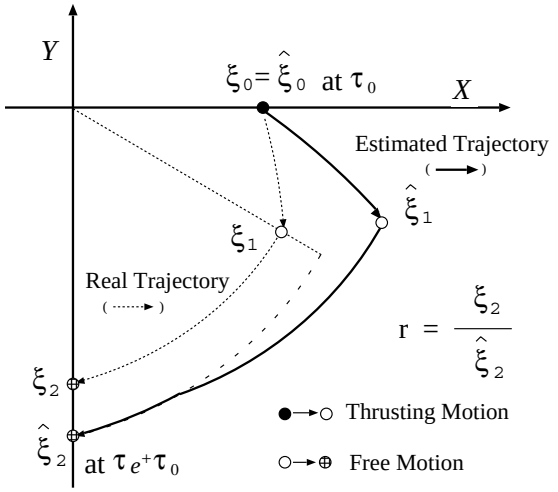

Fig. 15 Related to the relativity based on LOS Angle

The thrusting time τ_x and τ_y can be measured. The estimated state by EKF is denoted by $\hat{\boldsymbol{\xi}}$. We assume that the estimated state is equal to the real state at initial time, that is, $\hat{\boldsymbol{\xi}}_0 = \boldsymbol{\xi}_0$ in the section. However, if the actual thrust differs from the value in the model of EKF for the thrusting time, the state cannot be estimated successfully.

6.4 Thrust Estimation based on LOS Angles and Distance

During free motion, the state can be estimated successfully by EKF based on both LOS angles and distance. Thus, even if an error arises in the estimated state owing to the incorrect thrust value in the model of EKF during the velocity change, the error is corrected after free motion for long time as shown in Fig. 14. We assume that the estimated state just before the next thrusting motion becomes equal to the real state, that is,

$$\hat{\boldsymbol{\xi}}_2 \quad = \quad \boldsymbol{\xi}_2 \tag{20}$$

The real state just after the thrusting motion is represented as follows

$$\boldsymbol{\xi}_1 = \boldsymbol{A}(\tau_e - \tau_y)^{-1}\hat{\boldsymbol{\xi}}_2 \tag{21}$$

Substituting Eq.(21) into Eq.(19), the following relations are derived.

$$\boldsymbol{M}(\tau_x,\ \tau_y)\boldsymbol{\alpha} = \boldsymbol{A}(\tau_e - \tau_y)^{-1}\hat{\boldsymbol{\xi}}_2 - \boldsymbol{A}(\tau_y)\hat{\boldsymbol{\xi}}_0 \tag{22}$$

Solving the overdetermined linear equation(22) (two unknowns and four equations), the acceleration $\boldsymbol{\alpha}$ by the thrust can be estimated.

6.5 Thrust Estimation based on LOS Angles

As concluded in **Sec.5**, there is the problem that the estimated state for the free motion by EKF based on LOS Angles converges into an incorrect state geometrically similar to the real state in case of bad initial estimation. Thus, if an error arises in the estimated state owing to the incorrect thrust value in the model of EKF during the velocity change, the estimated state converges into the incorrect value after the free motion for long time as shown in Fig. 15. Therefore, we propose a method of estimating the state based on the characteristic that the estimated state converges to the similarity relation of the real state. At the time just before the next thrusting motion, it is assumed that the estimated state is similar to the real state in ratio r.

$$r\hat{\boldsymbol{\xi}}_2 \quad = \quad \boldsymbol{\xi}_2 \tag{23}$$

The real state just after the thrusting motion is represented as follows.

$$\boldsymbol{\xi}_1 = r\boldsymbol{A}^{-1}(\tau_e - \tau_y)\hat{\boldsymbol{\xi}}_2 \tag{24}$$

Substituting Eq.(24) into Eq.(19), the following relations are derived.

$$\overline{\boldsymbol{M}}(\tau_x,\ \tau_y)\begin{bmatrix} \boldsymbol{\alpha} \\ r \end{bmatrix} = -\boldsymbol{A}(\tau_y)\hat{\boldsymbol{\xi}}_0 \tag{25}$$

where

$$\begin{aligned} \overline{\boldsymbol{M}}(\tau_x,\ \tau_y) \quad &= \quad \left[\ \boldsymbol{M}(\tau_x,\ \tau_y) \ \vdots\ -\boldsymbol{A}^{-1}(\tau_e - \tau_y)\hat{\boldsymbol{\xi}}_2\ \right] \\ &\in \quad \boldsymbol{R}^{4\times 3} \end{aligned}$$

Solving the overdetermined linear equation(25) (three unknowns and four equations), the acceleration by the acceleration $\boldsymbol{\alpha}$ and the similarity ratio r can be estimated. Since the similarity ratio is estimated in Eq.(25), the problem that small steady deviation remains between the estimated trajectory and the real trajectory can be removed. Whenever the thrust is estimated, the estimated state by EKF based on LOS angles is also correctable with the similarity ratio r.

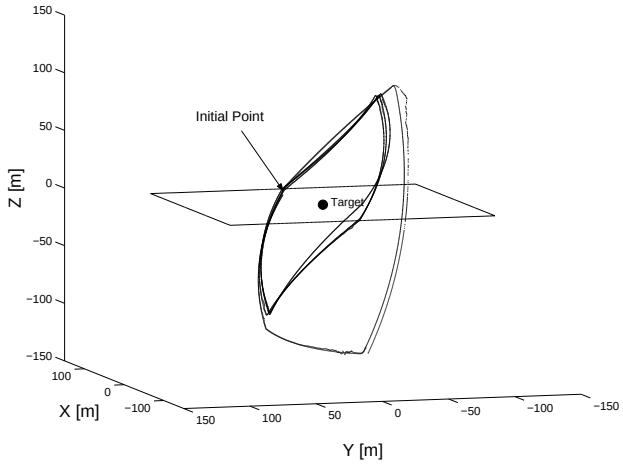

Fig. 16 4-Impulse Flyaround Trajectory Simulation (U_x = 20 [N], U_y = 20 [N], U_z = 20 [N])

7 Simulation

The proposed impulse flyaround and its control method is tested in simulation. Using this system, simulation is carried out under the condition that T/ω=0.1[s], the radius of earth orbit of the target is 6900 [km], mass of the chaser is 500[kg], and the initial position of chaser is $(x,\ y,\ z) = (100,\ 0,\ 0)$[m]. Let us define nominal thrusting force $U_x = U_y = U_z$ =20[N] in the direction of X, Y, and Z axes respectively. Under the situation that actual thrusting force is 90% to the nominal and falls to 50% suddenly after 3500[s], simulation is carried out. Desired trajectory is shown in Fig. 7. Result of the trajectory is shown in Fig. 16, Fig. 17, and Fig. 18, and result of the similarity ratio and the estimated thrust is shown in Fig. 19. The proposed system maintains the flyaround trajectory well.

8 Conclusion

In this paper, we propose control method in consideration of a change in the thrust. When a change in the thrust, the problem to produce were verified because of the extended Kalman filter which observe only two LOS angles. As the concept of the similarity ratio was introduced, the problem was solved and the thrust of the chaser can be estimated. The effectiveness is tested by integrated simulation including EKF, LQR, and VIC.

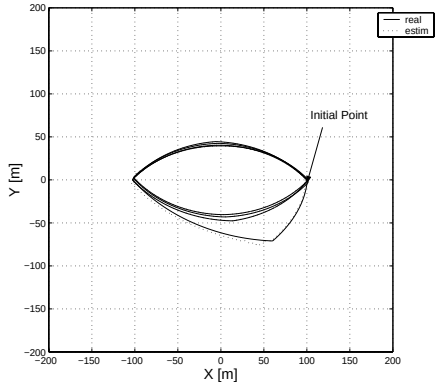

Fig. 17 X-Y Plane : 4-Impulse Flyaround Trajectory Simulation

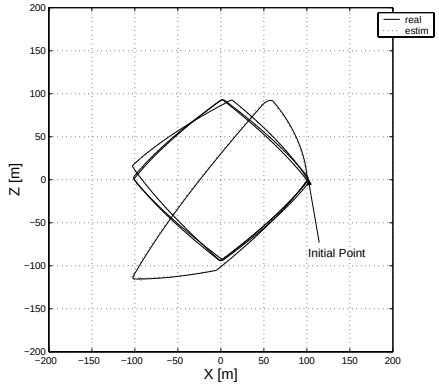

Fig. 18 X-Z Plane : 4-Impulse Flyaround Trajectory Simulation

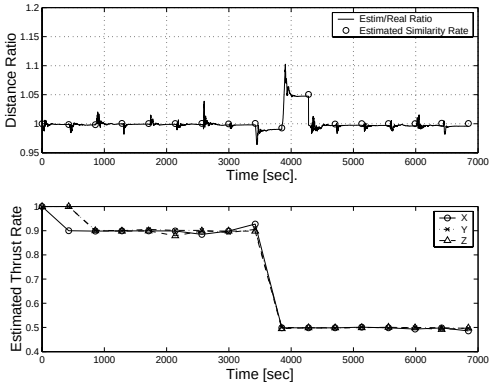

Fig. 19 Similarity ratio and Estimated thrust

References

[1] Howie Choset, David Kortenkamp, "Path Planning And Control for Free-Flying Inspection Robot In Space", Journal of Aerospace Engineering, April, 1999.

[2] K. Grim and C.R. Price, " Autonomous EVA Robotic Camera (AeRCAM) Sprint", In Advanced Developments in Space Robotics, AIAA Robotics Technology Forum, Aug 1-2 1996, Madison WI, Aug 1996.

[3] WWW page on Eyeball Satellite `http://giken.tksc.nasda.go.jp/Group/sentan/eyeball.html`

[4] Y.Masutani, M.Matsushita, and F.Miyazaki, "Flyaround Maneuvers on a Satellite Orbit by Impulsive Thrust Control", Proc. IEEE International Conference on Robotics and Automation, pp. 421–426, 2001.